Chemical Science

Accepted Manuscript

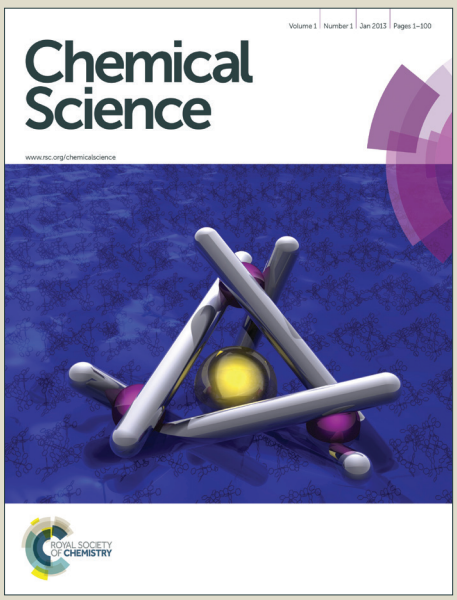

ROYAL SOCIETY OF CHEMISTRY

www.rsc.org/chemicalscience

Journal Name

RSCPublishing

ARTICLE

Ultrathin g-C_3N_4 /TiO_2 composites as photoelectrochemical elements for real-time evaluation of global antioxidant capacity†

Cite this: DOI: 10.1039/x0xx00000x

Received 00th January 2012,
Accepted 00th January 2012

DOI: 10.1039/x0xx00000x

www.rsc.org/

Weiguang Ma[a,b], Dongxue Han[a,b]*, Min Zhou[a,b], Hao Sun[c], Lingnan Wang[a,b], Xiandui Dong[a,b] and Li Niu[a,b]*

The antioxidants in biological organisms can scavenge excess free radicals and effectively reduce oxidative stress, which will further protect DNA, protein and lipid in human body from damaging and thus avoid inducing diseases. Therefore it is particularly significant to assay the antioxidant capacity of our habitual foods during diet valuation. Herein, ultrathin graphitic carbon nitride (utg-C_3N_4)/TiO_2 composites has firstly been introduced as sensing elements into a photoelectrochemical platform with a thin layer structured flow-cell for real-time assaying global antioxidant capacity in practical samples. In this system, the two-dimensional utg-C_3N_4 nanosheets/TiO_2 nano-particles composite material endowed much better optoelectronic function than that of individual material. In comparison with previous reports, this photoelectrochemical strategy shows considerable advantages including excellent anti-interference, high stability and reproducibility, and it is also proved as the most prompt, convenient and cost-effective method for antioxidant capacity detection till now. Moreover, utilizing theoretical and experimental examinations, we elaborately revealed its photoelectrochemical sensing mechanism. It is proposed that the developed method paves a first way to excellent antioxidant assays with advantages of photoelectrochemistry and fluidic cell and is expected to be further applied in food quality inspection, health guide as well as other fields.

Introduction

High concentration of free radicals will induce Oxidative Stress, which can further damage DNA, protein and lipid in organism, and leading to serious diseases such as Alzheimer, Parkinson, Cancer, etc.[1] Antioxidants, which are extensively exist in foods, can effectively scavenge free radical and protect organism maintaining in a healthy state[2]. Therefore, it is of significant importance to assay the antioxidant capacity in foods. At present, several methods have been developed for evaluation of antioxidants including chromatography [3], spectrophotometry [4] and electrochemical methods [5]. Although great progress has been achieved within these methods, several problems still need to be resolved: i) with chromatographic method, it is concentration of individual antioxidant but not global antioxidant capacity of the detected system that is determined; ii) the results are frequently interfered by the inherent foods colour during detection process while spectral methods are applied; iii) the work electrode is apt to be fouled by the production, which will seriously affect the following detection via the electrochemical method. To solve these problems, therefore, a preferable method with properties of rapidly response, high stability and excellent anti-interference should be urgently developed towards detection of antioxidation capacity in foods.

Bearing the fact in mind, herein, a photoelectrochemical

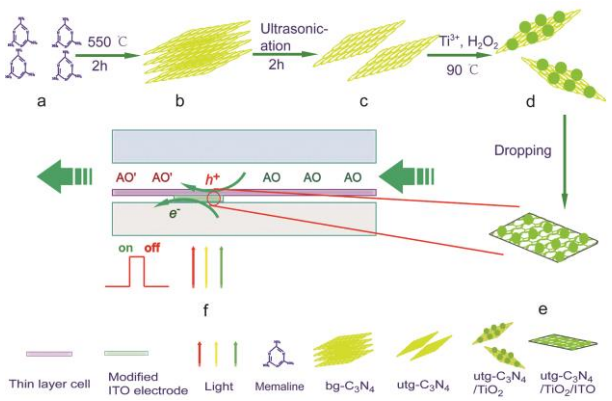

Fig. 1 Synthesis of utg-C_3N_4/TiO_2 (a~e) and illustration of thin layer photoelectrochemical flow cell (f). AO: antioxidants and AO•: oxidized antioxidants.

platform has been designed with ultrathin graphitic carbon nitride/titanium dioxides components (utg-C_3N_4/TiO_2) serving as photoelectrochemical elements for assaying antioxidant capacity in foods (Scheme in Fig. 1). As is well known that, material with good optoelectronic property plays a key role in an excellent photoelectrochemical platform. Although TiO_2 has a lot of remarkable properties such as good photostability, chemical/biological inert nature, nontoxicity and high electronic mobility, the performance of pristine TiO_2 will not sufficiently meet the needs of an ideal photoelectrochemical platform [6]. Inorganic semiconductors (such as CdS, ZnS, MoS_2) were used to functionalize TiO_2 for improving its properties due to their narrow bandgap[7] . However, the toxicity and corrosion limited their further application. Owing to outstanding properties including metal-free, nontoxicity, narrow bandgap, and easily processing for desired shapes [8], graphitic carbon nitride (g-C_3N_4) has been widely explored by many researchers [9]. In the g-C_3N_4/TiO_2 composites, due to proper band level between g-C_3N_4 and TiO_2, the photo-generated electron and hole can be easily separated, resulting in great improvement of photocatalytic activity. Concerning upon previous reports, the g-C_3N_4/TiO_2 composites have been synthesized for hydrogen evolutions and environmental purifications [10]. Yet, bulk g-C_3N_4 materials with low specific surface area and poor solubility were used in these researches, which have limited its potoelectrochemical properties. Luckly, g-C_3N_4 nanosheets with atomic-scale thickness can greatly promote photoresponse in contrast with bulk materials due to its high specific surface area [9b, 11]. A fully exposed surface of the ultrathin g-C_3N_4 (utg-C_3N_4) nanosheets makes it possible to utilize all the surface active sites. Recent theoretical investigations also revealed that utg-C_3N_4 nanosheets exhibited unique electronic and optical properties [11]. In this work, utg-C_3N_4/TiO_2 composites were synthesized via a simple method. Compared to g-C_3N_4/TiO_2, the photoelectrochemical properties of utg-C_3N_4/TiO_2 are greatly improved. By employing utg-C_3N_4/TiO_2 composites as photoelectrochemical elements, a thin layer flow cell has been designed and the resulting system demonstrated a series of advisable properties such as rapid response, anti-fouling and colour-interference-proof. These important features finally realized the real-time antioxidant capacity assay in foods (e.g. tea, coffee, etc.).

Results and discussion

The chemical synthesis route for the utg-C_3N_4/TiO_2 nanocomposite is illustrated in Fig. 1. Typically, bulk g-C_3N_4 (bg-C_3N_4) was first synthesized *via* thermal polycondensation of melamine at 550 ℃ according to previous literatures [12]. Thereafter, the obtained bg-C_3N_4 was ultrasonicated for 2h in water and utg-C_3N_4 nanosheets with a few layers were obtained. Cross-sectional atomic force microscopy (AFM) was further conducted to investigate the structural features of utg-C_3N_4 nanosheets (Fig.2a). The randomly measured nanosheets demonstrated very close thickness of ~1.2 nm (Fig.2b). This indicated that the exfoliated nanosheets were comprised of less

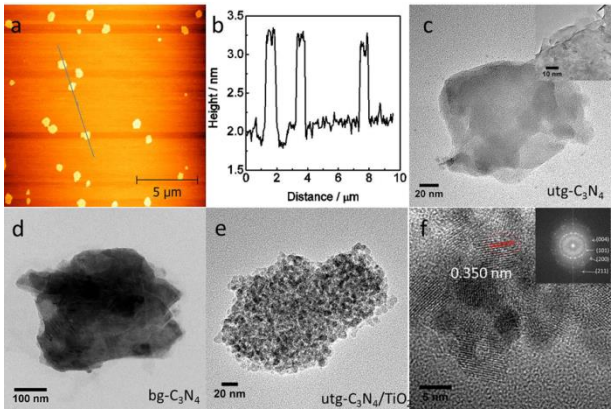

Fig. 2 AFM image of utg-C_3N_4 (a) and the corresponding height image of utg-C_3N_4 (b);TEM image of utg-C_3N_4 (c), bg-C_3N_4 (d) and utg-C_3N_4/TiO_2 (e); HRTEM of utg-C_3N_4/TiO_2 (f) and its fast Fourier transform (FFT) of image insert of (f); The insert of (c) is HRTEM image of utg-C_3N_4.

than five C-N layers, which is much thinner than those of reported [9b, 11]. TEM image of utg-C_3N_4 also showed similar results (Fig.2c). Different from bg-C_3N_4, the utg-C_3N_4 nanosheets can be very well dispersed in water and the suspension can even stay for a few weeks without aggregation (Fig. S2, EIS†). Finally, c.a. 10nm TiO_2 nanoparticles were uniformly decorated onto the as prepared utg-C_3N_4 nanosheets (Fig. 2e) *via* a self-assembly process. High-resolution TEM (HRTEM) analysis revealed the highly crystalline feature of TiO_2 nanoparticles with a lattice spacing of 0.350 nm (Fig. 2f), which can be assigned to the (101) plane of anantase TiO_2 [13].

X-ray diffraction (XRD) patterns of bg-C_3N_4, utg-C_3N_4 nanosheets, and utg-C_3N_4/TiO_2 nanocomposites were shown in Fig. 3a, respectively. For bg-C_3N_4, the strong XRD Bragg peak at 27.7 ° is attributed to the characteristic interlayer stacking reflection of conjugated aromatic systems, indexing for graphitic materials as the (002) peak[8b]. After exfoliation, the intensity of the (002) peak significantly decreased (Fig. 3a), which demonstrated that the layered g-C_3N_4 has been successfully exfoliated into layer structures as expected [9b]. The Bragg peaks corresponding to TiO_2 and utg-C_3N_4 nanosheets were also observed simultaneously in Fig. 3a, which indicated that the consolidated structure of utg-C_3N_4/TiO_2 components have been obtained successfully [13]. X-ray photoelectron spectroscopy (XPS) measurements and elemental analysis were performed to probe the chemical composition of utg-C_3N_4 and utg-C_3N_4/TiO_2. As shown in Fig. 3b, the utg-C_3N_4 nanosheets sample exhibited C1s and N1s signals with a C/N ratio of 1.31, which is very close to the ideal g-C_3N_4 composition (C/N 1.33) [9b], indicating that the chemical composition and the coordination of carbon and nitrogen in utg-C_3N_4 were retained during the liquid exfoliation process. High-resolution spectra of C1s (Fig. 3c) at 285.5eV and N1s (Fig. 3d) at 398.5 eV are assigned to the sp2 C=N bond in the s-triazine ring. The peaks at 288.3 eV and 284.6 eV in the C1s zone are attributed to electrons originating from a sp2 C atom attached to a -NH_2 group and to an aromatic carbon atom. The contribution at 399.5 and 401.2 eV in the N1s zone are ascribed to N atoms

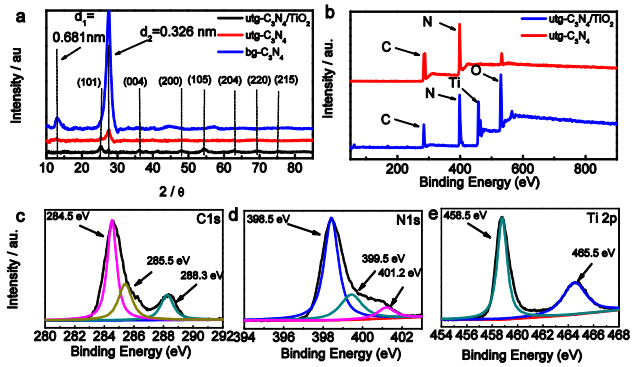

Fig. 3 XRD of bg-C_3N_4, utg-C_3N_4 and utg-C_3N_4/TiO_2 (a); XPS of utg-C_3N_4 and utg-C_3N_4/TiO_2 (b); High-resolution C1s (c) and N1s of utg-C_3N_4 (d); High-resolution Ti2p of utg-C_3N_4/TiO_2 (e).

that are bound to three C atoms; these N atoms are located in the heptazine ring and as bridging atom, respectively. After dispersion of TiO_2 nanoparticles on the utg-C_3N_4, Ti2p and O1s were observed in Fig. 3b. The High-resolution spectra of Ti2p (Fig. 3e) at 458.5 eV and 465.5 eV demonstrated that Ti present four valence [14]. All the above results indicated that utg-C_3N_4/TiO_2 has been successfully synthesized. More evidences for the structural properties investigations of the utg-C_3N_4/TiO_2 composites from UV-vis and FTIR were presented in the Supporting Information (Fig. S3-S4, EIS†)

Photoelectrochemical measurements have attracted tremendous attention due to combined merits of both optical and electrochemical methods [15], in which optoelectronic materials play a key role during the essential photocatalysis. As shown in Fig. 4a, pristine TiO_2 modified electrode exhibited a weak photocurrent response (19.38 nA, curve a_0) owning to its poor absorption in visible light (Fig. S3a, EIS†). While after introducing of bg-C_3N_4, the photocurrent greatly increased to

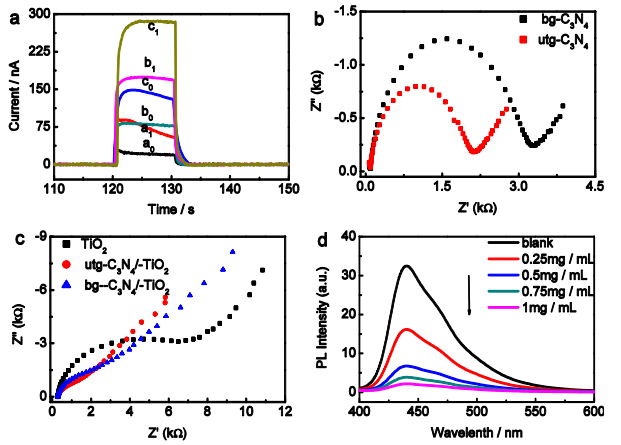

Fig. 4 Photocurrent responses of TiO_2 (a0, a1), bg-C_3N_4/TiO_2 (b0, b1) and utg-C_3N_4/TiO_2 (c0,c1) modified ITO without (a0, b0, c0) and with (a1, b1, c1) 50 μmol•L^{-1} CT (a); EIS images of bg-C_3N_4 and utg-C_3N_4 (b); EIS images of TiO_2,bg-C_3N_4 /TiO_2 and utg-C_3N_4 /TiO_2 (c) in mixed solution of 5 mmol•L^{-1} $[Fe(CN)_6]^{3-/4-}$ and 0.1 mol•L^{-1}KCl aqueous solution; Fluorescence emission of utg-C_3N_4 (d) water solution with different concentration of TiO_2 at excitation 315 nm. (The work electrode of (b) is glassy carbon electrode at open circular potential without light; the work electrode of (c) is ITO at 0.3 V vs Ag /AgCl under light.).

76.85 nA (curve b_0), since bg-C_3N_4 can be efficiently excited under visible light radiation (Fig. S3a, EIS†) and resulted in a much stronger photocurrent response. To our surprise, when utg-C_3N_4 was applied instead of bg-C_3N_4 in the composites material, it showed a distinctly enlarged photocurrent which was ca. 1.7 times larger than that of bg-C_3N_4/TiO_2 modified electrode. This excellent photoelectrochemical prosperity might be attributed to the following reasons: i) utg-C_3N_4 presents better conductivity than that of bg-C_3N_4 (Fig. 4b); ii) TiO_2 nanoparticles can disperse more uniformly onto the utg-C_3N_4 sheets (Fig. 2e) in comparison with bg-C_3N_4 (Fig. S5, EIS†), which will greatly promote the electron transfer between TiO_2 nanoparticle and utg-C_3N_4, and thus efficiently reduce recombinations between electron and hole. As shown in Fig. 4c, the charge-transfer resistance of utg-C_3N_4/TiO_2 is 658.6 Ω•cm^2, which is much smaller than that of bg-C_3N_4/TiO_2 (1429.0 Ω•cm^2) under visible radiation. This smaller arc radius implies a much higher efficiency of charge transfer. In the fluorescence quenching experiment, the fluorescence intensity of utg-C_3N_4 is observed gradually decreased at 440 nm with the increasing of TiO_2 concentration (Fig. 4d), for the recombination between electron and hole was suppressed [16]. As shown in Fig. 4a, upon the addition of 50 μmol•L^{-1} catechin (CT, a typical example of antioxidants), the photocurrents on all these three modified electrodes increased as expected, which can be attributed to the oxidization of CT by the holes. Among those cases, utg-C_3N_4/TiO_2 exhibited the largest photocurrent (284.28 nA), which was about 5.1 and 1.7 times greater than those of pristine TiO_2 and bg-C_3N_4/TiO_2, respectively. Other antioxidants also showed obvious signal on the utg-C_3N_4/TiO_2 modified electrode. Therefore, utg-C_3N_4/TiO_2 nanocomposite material seems to be an advisable candidate for antioxidant capacity assay.

Upon the developing of antioxidants capacity detection device, a kind of static cell has been firstly introduced (Fig. S6a, EIS†). By using this device, although photoelectrochemical assay could be realized and excellent responses obtained towards various antioxidants, however, the utg-C_3N_4/TiO_2-modified electrode was easily fouled during successive electrochemical measurements (Fig. S7a, EIS†). In order to improve the recyclability of photocatalyst, a flow photoelectrochemical cell with thin layer structure was then developed to replace previous static cell (Fig. 5a, Fig. S6b and Fig. S6c, EIS†). Such a flow photoelectrochemical cell shows specific properties as high mass diffusion and depletion. With only a very small amount of sample requirement, strong signals and high detection sensitivity [17] could be obtained. Just as expected, the photocurrent is quite stable even after a long time running in such a flow photoelectrochemical cell (Fig. S7b, EIS†), which has successfully guaranteed the recyclability of the photocatalyst and made this device an excellent candidate for the real-time evaluation of antioxidant capacity. Just as shown in Fig. S8 (EIS†), when the photoelectrochemical assay was carried out, 0 V has been selected since simultaneous advisable sensitivity and anti-interference can be achieved at this potential. Then, antioxidant capacities of nine typical

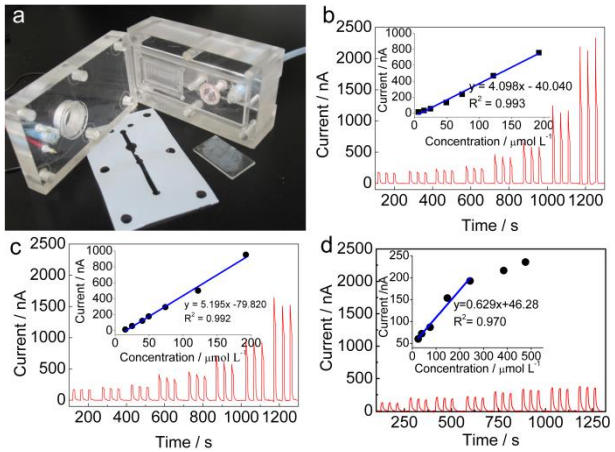

Fig. 5 The photograph of thin layer photoelectrochemical flow cell (a); concentration-dependent photocurrent of different antioxidants (CA b), CT c) and AA d)). (The insert in b, c, d are linear curves of CA, CT and AA, respectively.)

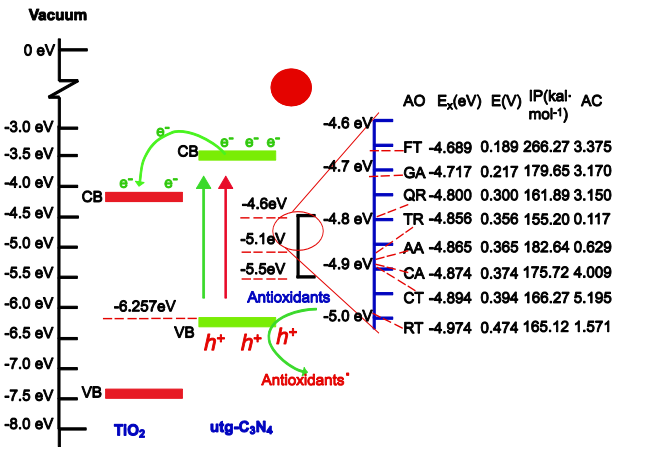

Fig. 6 Mechanism of the photoelectrochemical sensor for detection of antioxidant capacity. AO: antioxidant, Ex (eV): the redox potential of antioxidants with respect to vacuum, E (V): the redox potential of antioxidants (vs Ag/AgCl), IP (kcal•mol^{-1}): ionization potential of antioxidants, AC: antioxidant capacity obtained from slope of standard calibration curve of each antioxidant.

antioxidants were successfully detected including Quercetin (QR), Gallic acid (GA), Caffeic acid (CA), Catechin (CT), Fisetin (FT), Rutin (RT), Trolox (TR), Ascorbic acid (AA) and Glutathione (GSH). As shown in Table S1 (EIS†), all of these nine antioxidants exhibited good responses with wide linear range. Among them, the relationships between photoelectrocurrent and concentrations of CA, CT and AA are shown in Fig. 5, whose linear concentration range depicted as 15.00~193.31 μmol•L^{-1}, 24.96~192.31 μmol•L^{-1} and 25.00~243.09 μmol•L^{-1} respectively, and their relative standard deviation (RSD, %) are 4.6%, 3.2% and 5.6%. It is noticeable that, even after continually used for two weeks, such photoelectrochemical sensors could still remained at least 95% of initial detection signals, which indicated that the fouling of photocatalyst could be weakened to a great extent within such a thin layer photoelectrochemical flow cell system.

Theoretically, two main mechanisms have been proposed including hydrogen atom transfer and single electron transfer during the reaction process of antioxidants species [18]. As shown in Fig. 6, the valence band (VB) of utg-C_3N_4 is proved to be -6.257 eV obtained from Mott-Schottky (Fig. S9, EIS†) and UV-vis diffuse reflectance spectra (Fig. S3b, EIS†), which is much higher than the oxidation of H_2O (-5.30 eV)[8b]. Usually, when water is oxidized, hydroxyl radicals will generate [19], however, in this system the fluorescence peak at 425 nm could not be observed in solution containing terephthalic acid and utg-C_3N_4/TiO_2 under visible light irritation at various durations (Fig. S10, EIS†), which indicated that no hydroxyl radical was produced in our case [5e]. Therefore, such a photoelectrochemical approach for antioxidant capacity assay by using utg-C_3N_4/TiO_2 as photocatalyst is ascribed to be an electron transfer process. The detailed mechanism can be proposed as: when utg-C_3N_4 was excited by visible light irritation, electron (e^-) and hole (h^+) generated, and an immediate electron transfer to the conduction band (CB) of TiO_2 occurred followed by a prompt electron arriving at the ITO substrate, thus lead to generation of photocurrent. While with the introducing of antioxidants, h^+ of utg-C_3N_4 could be refilled by electrons from antioxidants and these occupied holes were ready for the next excitation. This process could significantly enhance the photocurrent. Therefore, we believe that based on single electron transfer reactions, the regeneration ability of h^+ and e^- transfer in utg-C_3N_4/TiO_2 nanocomposite during antioxidants reactions should be defined as a comprehensive antioxidants capacity evaluation but not a simple concentration detection of antioxidants.

As shown in Fig. 6, CT, CA, FT, GA, QR, and RT showed amazing antioxidant capacity with contrast to TR, AA and GSH. Since the mechanism of the present photoelectrochemical sensor was based on electron transfer reaction, the stronger the antioxidant capacity is, the easier for it to lose electron. In order to clarify antioxidant capacity of different kinds of antioxidants, detailed reaction process between photocatalyst and antioxidants under light radiation have been thoroughly investigated. First, ionization potential of individual antioxidant was estimated using B3LYP/6-311G (d,p) method through theoretical structural simulation of each antioxidant molecule, since the ionization potential is the most significant energetic factor for antioxidants capacity evaluation[18b]. It is observed from Fig. 6, most of the phenols samples, for example, CT, CA, FT, GA, QR, and RT have relatively low ionization potential and show strong antioxidant capacities[18c]. This conclusion can also be proved by the calculated results of L-cysteine and glucose, which do not exhibit interference with our detection of antioxidant capacity in food (Fig. S12, EIS†) due to their high ionization potential (187.95 kcal•mol^{-1} and 191.17 kcal•mol^{-1}). But GA and TR are disputable by this explanation. So other factors should be considered here besides the ionization potential. The redox potentials of antioxidants on the glassy carbon electrode were so determined, which is also a key role for evaluation of antioxidant capacity [5a, 20]. As expected, GA showed low redox potential and high antioxidant capacity. Compared to GSH, other phenols also presented low redox potential (Fig. S11, EIS†) and high antioxidant capacity. It is

Table 1 The results of antioxidant capacity for Teas (T) and Coffee (C) with our photoelectrochemical sensor, Folin–Ciocalteu method and DPPH method, respectively.

Practical Samples	*Photoelectroche-mical Sensor (mg/g GA)*	*Folin-Ciocalteu Method (mg/g GA)*	*DPPH Method (mg/g TROLOX)*
T_1	72.212 ±0.612	62.190 ±0.426	163.610 ±0.925
T_2	95.860 ±0.536	88.610 ±0.731	227.880 ±0.834
T_3	21.010 ±0.214	23.270 ±0.198	113.600 ±0.736
T_4	30.570 ±0.165	34.960 ±0.767	132.560 ±0.961
C_1	3.334 ±0.068	9.020 ±0.213	14.740 ±0.346
C_2	3.759 ±0.086	9.645 ±0.324	15.490 ±0.425
C_3	1.937 ±0.034	5.520 ±0.228	6.890 ±0.123
C_4	2.353 ±0.056	6.830 ±0.621	9.682 ±0.456

suggested that effect of molecular structure also plays a key role in this photoelectrochemical reaction. Theoretical analysis indicated that the number and position of the hydroxyl groups, as well as the degree of conjugation of the entire molecule, can also affect the antioxidant capacity assay [21]. Since CT, FT, QR, and RT present two ortho-hydroxyl groups, they showed stronger antioxidant capacity with contrast to TR. The contact mode between antioxidants and photocatalyst is another important factor during the reaction. The utg-C_3N_4 has a π-conjugated structure, which can easily induce adsorption of the benzene structured antioxidants through π-π interaction and then promote electron transfer [8b]. Considered all the above factors, it is concluded that phenol antioxidants, such as CT, CA, FT, QR, GA and RT, should show higher antioxidant capacity, while TR, AA and especially GSH might present lower antioxidant capacity, which was similar to the optical method [4c].

The anti-interference characters of this photoelectrochemical sensor have been further investigated. A typical antioxidant system, as an example, has been studied which is containing 25 μmol•L^{-1} GA as well as some possible interference species commonly found in food and drinking (shown in Fig. S12, EIS†). Just as shown, 1000 times of L-proline, L-glycine, L-histidine, ethanol, methanol, 500 times of L-threonine, fructose, glucose, L-citric acid, L-malic acid and 20 times of L-cysteine did not lead to distinct interference with the results of antioxidant capacity assay with our photoelectrochemical sensor. These results further confirmed that the present photoelectrochemical sensor can be applied in the practicable complex conditions for antioxidant capacity evaluation.

Actually, by using this photoelectrochemical sensor, antioxidant capacity of four brands of commercial tea and four brands of commercial coffee were examined. Compared to coffee, all the tea samples presented higher antioxidant capacities (Table 1), and all these results were found consistent well with the results by both Folin-Ciocalteu (F-C) and DPPH methods. The detection data of coffee obtained by our photoelectrochemical measurement is smaller than that of F-C method, which should be assigned to the possible interference of the natural coffee and reducing sugars colours by F-C method [22]. Here, in our photoelectrochemical detection system, the utg-C_3N_4/TiO_2 components modified ITO electrode was irradiated from the backside, which can completely avoid such colour interferences during the antioxidant capacity determinations. Therefore, the results of such a novel photoelectrochemical sensor would be more close to the true values.

Conclusions

In summary, as an excellent optoelectronic material, utg-C_3N_4/TiO_2 composites have been designed and applied in a thin layer structured photoeletrochemical flow cell to detect antioxidant capacity in food. Detailed studies have unambiguously revealed that, besides advantaged including rapid response, high sensitivity, long time stability and little sample requirement, this photoeletrochemical platform can fully overcome three tough problems in antioxidant capacity assay (global antioxidant capacity determination, interference of sample colours and poison of work electrode). Furthermore, the mechanism of this photoeletrochemical sensor was elaborately explored based on single electron transfer reaction and the results are comparable with Folin-Ciocalteu and DPPH method. By using such a thin layer photoeletrochemical flow cell, the actual samples could be rapidly real-time detected. This novel method paves the way to high-performance antioxidant assay combining advantages of photoelectrochemistry and fluidic cell, which is expected to be further applied into analytical instruments for commercialization.

Acknowledgements

This work was supported by NSFC, China (21225524, 21205112 and 21175130).

Notes and references

[a] State Key Laboratory of Electroanalytical Chemistry, c/o Engineering Laboratory for Modern Analytical Techniques, Changchun Institute of Applied Chemistry, Chinese Academy of Sciences, Changchun, Jilin 130022 (P. R. China). E-mail: dxhan@ciac.ac.cn, lniu@ciac.ac.cn, Fax: (+)86-431-85262800, Tel: (+)86-431-85262425.

[b] Graduate University of Chinese Academy of Sciences, Chinese Academy of Sciences, Beijing 100039 (P. R. China)

[c] College of chemistry, Northeast Normal University, Changchun, Jilin 130022(P. R. China).

† Electronic Supplementary Information (ESI) available: Detailed materials and methods; SEM, UV-vis DRS, FTIR spectra; dispersion of bg-C_3N_4 and utg-C_3N_4 in water; the digital imagines of the static cell and thin layer structured photoelectrochemical flow cell; stability of static cell and flow cell; potential optimization; Mott-Schottky plot; fluorescence emission spectra; CV of antioxidants; interference detection; linear equations, correlation coefficients, redox potential, ionization potential, antioxidant capacity and linear ranges for antioxidants. See DOI: 10.1039/b000000x/

[1] a)K. Irani, Y. Xia, J. L. Zweier, S. J. Sollott, C. J. Der, E. R. Fearon, M. Sundaresan, T. Finkel, P. J. GoldschmidtClermont, *Science* **1997**,

275, 1649-1652; b)T. Finkel, N. J. Holbrook, *Nature* **2000**, *408*, 239-247; c)R. M. Perera, N. Bardeesy, *Nature* **2011**, *475*, 43-44.

[2] a)R. Mittler, *Trends Plant Sci.* **2002**, *7*, 405-410; b)Y. S. Velioglu, G. Mazza, L. Gao, B. D. Oomah, *J. Agr. Food Chem.* **1998**, *46*, 4113-4117; c)M. V. Eberhardt, C. Y. Lee, R. H. Liu, *Nature* **2000**, *405*, 903-904.

[3] a)M. Bedner, D. L. Duewer, *Anal. Chem.* **2011**, *83*, 6169-6176; b)H. M. Merken, G. R. Beecher, *J. Agr. Food Chem.* **2000**, *48*, 577-599; c)A. Pukalskas, T. A. van Beek, P. de Waard, *J. Chromatogr. A* **2005**, *1074*, 81-88.

[4] a)R. L. Prior, X. L. Wu, K. Schaich, *J. Agr. Food Chem.* **2005**, *53*, 4290-4302; b)M. Ozyurek, K. Guclu, R. Apak, *Trac-trend. Anal. Chem.* **2011**, *30*, 652-664; c)M. Ozyurek, N. Gungor, S. Baki, K. Guclu, R. Apak, *Anal. Chem.* **2012**, *84*, 8052-8059.

[5] a)P. A. Kilmartin, H. L. Zou, A. L. Waterhouse, *J. Agr. Food Chem.* **2001**, *49*, 1957-1965; b)A. G. Crevillen, M. Avila, M. Pumera, M. C. Gonzalez, A. Escarpa, *Anal. Chem.* **2007**, *79*, 7408-7415; c)M. Fatima Barroso, N. de-los-Santos-Alvarez, C. Delerue-Matos, M. B. P. P. Oliveira, *Biosens. Bioelectron.* **2011**, *30*, 1-12; d)R. Oliveira, F. Bento, C. Sella, L. Thouin, C. Amatore, *Anal. Chem.* **2013**; *85*, 9057-9063; e)J. F. Liu, C. Roussel, G. Lagger, P. Tacchini, H. H. Girault, *Anal. Chem.* **2005**, *77*, 7687-7694; f)J. Liu, B. Su, G. Lagger, P. Tacchini, H. H. Girault, *Anal. Chem.* **2006**, *78*, 6879-6884.

[6] A. Fujishima, K. Honda, *Nature* **1972**, *238*, 37-38.

[7] L. Zhang, H. Cheng, R. Zong, Y. Zhu, *J. Phys. Chem. C* **2009**, *113*, 2368-2374.

[8] a)Y. Zhang, A. Thomas, M. Antonietti, X. Wang, *J. Am. Chem. Soc.* **2009**, *131*, 50-51; b)X. Wang, K. Maeda, A. Thomas, K. Takanabe, G. Xin, J. M. Carlsson, K. Domen, M. Antonietti, *Nat. Mater.* **2009**, *8*, 76-80; c)J. Zhang, X. Chen, K. Takanabe, K. Maeda, K. Domen, J. D. Epping, X. Fu, M. Antonietti, X. Wang, *Angew. Chem. Int. Ed.* **2010**, *49*, 441-444.

[9] a)S. Yang, X. Feng, X. Wang, K. Muellen, *Angew. Chem. Int. Ed.* **2011**, *50*, 5339-5343; b)S. Yang, Y. Gong, J. Zhang, L. Zhan, L. Ma, Z. Fang, R. Vajtai, X. Wang, P. M. Ajayan, *Adv. Mater.* **2013**, *25*, 2452-2456; c)Z. Tang, X. Chen, H. Chen, L. Wu, X. Yu, *Angew. Chem. Int. Ed.* **2013**, *52*, 5832-5835; d)Y. Wang, X. Wang, M. Antonietti, *Angew. Chem. Int. Ed.* **2012**, *51*, 68-89; e)Y. Chen, J. Zhang, M. Zhang, X. Wang, *Chem. Sci.* **2013**, *4*, 3244-3248.

[10] a)X. Zhou, B. Jin, L. Li, F. Peng, H. Wang, H. Yu, Y. Fang, *J. Mater. Chem.* **2012**, *22*, 17900-17905; b)B. Chai, T. Peng, J. Mao, K. Li, L. Zan, *Phys. Chem. Chem. Phys.* **2012**, *14*, 16745-16752; c)C. Miranda, H. Mansilla, J. Yanez, S. Obregon, G. Colon, *J. Photochem. Photobiol. A* **2013**, *253*, 16-21.

[11] X. Zhang, X. Xie, H. Wang, J. Zhang, B. Pan, Y. Xie, *J. Am. Chem. Soc.* **2013**, *135*, 18-21.

[12] Y. Cui, Z. Ding, X. Fu, X. Wang, *Angew. Chem. Int. Ed.* **2012**, *51*, 11814-11818.

[13] C. Chen, W. Cai, M. Long, B. Zhou, Y. Wu, D. Wu, Y. Feng, *ACS Nano* **2010**, *4*, 6425-6432.

[14] W. Ma, D. Han, N. Zhang, F. Li, T. Wu, X. Dong, L. Niu, *Analyst* **2013**, *138*, 2335-2342.

[15] a)V. Pardo-Yissar, E. Katz, J. Wasserman, I. Willner, *J. Am. Chem. Soc.* **2003**, *125*, 622-623; b)L. Sheeney-Haj-Khia, B. Basnar, I. Willner, *Angew. Chem. Int. Ed.* **2005**, *44*, 78-83; c)H. Li, J. Li, Z. Yang, Q. Xu, X. Hu, *Anal. Chem.* **2011**, *83*, 5290-5295; d)X. Zhao, S. Zhou, L.-P. Jiang, W. Hou, Q. Shen, J.-J. Zhu, *Chem.-Eur. J.* **2012**, *18*, 4974-4981; e)W. Ma, D. Han, S. Gan, N. Zhang, S. Liu, T. Wu, Q. Zhang, X. Dong, L. Niu, *Chem. Commun.* **2013**, *49*, 7842-7844.

[16] Y. Hou, A. B. Laursen, J. Zhang, G. Zhang, Y. Zhu, X. Wang, S. Dahl, I. Chorkendorff, *Angew. Chem. Int. Ed.* **2013**, *52*, 3621-3625.

[17] E. R. Montgomery, R. W. Murray, *Anal. Chim. Acta* **1996**, *321*, 195-199.

[18] a)J. S. Wright, E. R. Johnson, G. A. DiLabio, *J. Am. Chem. Soc.* **2001**, *123*, 1173-1183; b)M. Leopoldini, I. P. Pitarch, N. Russo, M. Toscano, *J. Phys. Chem. A* **2004**, *108*, 92-96; c)M. Leopoldini, T. Marino, N. Russo, M. Toscano, *J. Phys. Chem. A* **2004**, *108*, 4916-4922.

[19] H. S. Park, K. C. Leonard, A. J. Bard, *J. Phys. Chem. C* **2013**, *117*, 12093-12102.

[20] A. Rodrigues, A. C. S. Ferreira, P. G. de Pinho, F. Bento, D. Geraldo, *J. Agr. Food Chem.* **2007**, *55*, 10557-10562.

[21] C. A. RiceEvans, N. J. Miller, G. Paganga, *Free. Radical. Biol. Med.* **1996**, *20*, 933-956.

[22] a)N. Kovachev, A. Canals, A. Escarpa, *Anal. Chem.* **2010**, *82*, 2925-2931; b)M. Gamella, S. Campuzano, A. J. Reviejo, J. M. Pingarron, *J. Agr. Food Chem.* **2006**, *54*, 7960-7967.

